TASK-ORIENTED DYNAMIC MODELING OF TWO COOPERATING ROBOTS

R. Mattone, A. De Luca

Dipartimento di Informatica e Sistemistica (DIS)
Università di Roma "La Sapienza"
Via Eudossiana 18, 00184 Roma, Italy

mattone@labrob.ing.uniroma1.it adeluca@giannutri.caspur.it

ABSTRACT

We present a general formalism for deriving a control-oriented model of cooperating tasks for multi-robot systems and its specific application to a cell with two different robots involved in a mechanical finishing operation. The modeling approach is flexible enough so as to cover different possible interaction types between the end-effector of each robot and the common payload and can be easily applied even to complex cooperating tasks, as in the considered example. Since the interesting aspects and quantities needed for the correct execution of the task are intrinsically characterized, this description of robotic tasks is useful for control purposes.

KEYWORDS: Cooperating robots, Modeling, Force-motion control.

1. INTRODUCTION

Modeling and control of cooperating robots have been considered extensively in the literature (see, e.g., [1–3]). However, most papers are restricted by a common set of assumptions. In particular: the payload is a single rigid object; all robots have similar mobility; each robot rigidly grasps the payload (power grasp); the contact points are fixed in the object frame; no other environmental constraints are imposed on the payload. With these assumptions, the overall task description is obtained by coupling, through the exchanged contact forces, the dynamic model of the object with the dynamics of the multiple robots. From the control point of view, hybrid tasks are then defined in a direct way in terms of tracking the object motion and regulating the internal forces. The force/load distribution among the robots can be formulated as a optimization problem [4–5].

Indeed, the above modeling assumptions can be relaxed or generalized. Handling of a flexible object is analyzed in [6], while the case of payloads consisting of multiple rigid bodies is considered in [7]. Different grasping types have been classified using grasp matrices in [8]. In particular, point contacts are assumed in [9], where the coordination of robots pushing against a common object is studied. Much research is devoted to the case of rolling contacts (a nonholonomic constraint) in multi-fingered dextrous hands [10]. Whenever the grasp of a single robot does not determine completely the object pose, a model of the friction at the contact is also required. The analysis of this effect is usually performed in quasi-static conditions.

In the above works, specific robotic systems have been considered without using a unified modeling approach that could cover them altogether. This prevents a systematic generation of the governing equations and the general analysis of control aspects. On the other hand, in [11] we have started developing a task-based modeling approach of cooperating robots that complies with all the above open issues. The key point is a parametric description of the given task, with the introduction of suitable sets of task variables. As an example, general grasping conditions are explicitly characterized by means of kinematic variables describing the feasible relative motion in the robot-payload interaction. In this way, even moving contact points on the payload surface can be taken into consideration. Furthermore, specific variables can be defined along directions where friction (of any type) acts during dynamic operation.

Although the formalism can be extended so as to model the presence of external constraints, of rolling contacts, or of payload with extra degrees of freedom (see [7]), we limit here our analysis to the physical conditions occurring in the robotic cell used as a case study.

In the next section we briefly outline the modeling steps and the associated definition of kinematic, static, and dynamic quantities. An automatic decomposition of contact forces is provided, based on energy-transfer (and thus, unit invariant) arguments. Then, we apply our approach to a robotic cell constituted by a 4-dof SCARA robot arm and a 6-dof parallel platform (SmartEE).

2. COOPERATING ROBOTS-ENVIRONMENT MODEL

2.1 Kinematics

Consider a system of $m = 2$ robots with n_i joints ($i = 1, 2$) that cooperate in the execution of a task defined on a common payload, that may possibly be subject also to other environmental constraints. We assume that the contact between each robot and the payload is never lost and that, during the whole task execution, the contact points are either fixed or mobile. For the mobile contacts, the associated friction effects are considered explicitly.

Each manipulator configuration is identified by the joint variables vector $\mathbf{q}_i \in I\!R^{n_i}$, while its end-effector pose is given by a vector $\mathbf{p}_i \in I\!R^{g_i}$, being g_i the number of degrees of freedom (dofs) of motion of the ith robot end-effector. The end-effector pose collects the position $\mathbf{r}_i \in I\!R^{g_{r_i}}$ and a minimal representation of the orientation $\mathbf{o}_i \in I\!R^{g_{o_i}}$ (e.g., Euler angles if $g_{o_i} = 3$), where g_{r_i} and g_{o_i} respectively are the number of linear and rotational dofs of the ith robot end-effector and $g_i = g_{r_i} + g_{o_i}$. The end-effector velocity is $\mathbf{v}_i = (\dot{\mathbf{r}}_i, \omega_i) \in I\!R^{g_i}$, related to the time derivative $\dot{\mathbf{p}}_i$ of the pose by a matrix transformation depending in general on $\mathbf{o}_i$. Then, the end-effector kinematics is described *from the* i*th robot side* by

$$\mathbf{p}_i = \mathbf{k}_i(\mathbf{q}_i), \qquad \mathbf{v}_i = \mathbf{J}_i(\mathbf{q}_i)\dot{\mathbf{q}}_i, \qquad i = 1, 2, \tag{1}$$

where $\mathbf{J}_i(\mathbf{q}_i)$ is the geometric Jacobian of the ith robot.

Let l be the total number of parameters describing the payload dynamics and e the number of *extra dofs* that describe the payload dynamics when the contact points are kept fixed. Thus, $d = l - e$ will be the number of dynamic coordinates needed to characterize the grasp. Then, the payload configuration is identified by a set of generalized coordinates $\mathbf{s}_L \in I\!R^l$ (needed to describe the *environment* dynamics). Vector $\mathbf{s}_L$ splits in general in two vectors of generalized coordinates: $\mathbf{s}_{LE} \in I\!R^e$ for the extra dofs and $\mathbf{s}_{LD} \in I\!R^d$ that completes the description of the payload configuration and is necessary to characterize the grasp. From now on, we suppose that there are no extra dofs in the payload ($e = 0$). Depending on the type of contact between each robot and the object, other variables are in general necessary, in addition to $\mathbf{s}_{LD}$, to complete the description of the pose of the ith robot end-effector *from the environment side*. These variables describe the relative motion between the robots and the payload and may be partitioned in those on which the generalized friction forces at the contact perform work, $\mathbf{s}_{F_i} \in I\!R^{f_i}$ (*friction* variables), and those on which no work is performed by any force, $\mathbf{s}_{K_i} \in I\!R^{k_i}$ (*kinematic* variables). Then, we can write:

$$\mathbf{p}_i = \mathbf{\Gamma}_i(\mathbf{s}_{LD}, \mathbf{s}_{F_i}, \mathbf{s}_{K_i}), \qquad \mathbf{v}_i = \mathbf{T}_i(\mathbf{s}_{LD}, \mathbf{s}_{F_i}, \mathbf{s}_{K_i}) \begin{bmatrix} \mathbf{s}_{LD} \\ \mathbf{s}_{F_i} \\ \mathbf{s}_{K_i} \end{bmatrix}, \qquad i = 1, \ldots, m. \tag{2}$$

Matrix $\mathbf{T}_i$ can be partitioned as $\mathbf{T}_i = [\,\mathbf{T}_{D_i} \quad \mathbf{T}_{F_i} \quad \mathbf{T}_{K_i}\,]$, expliciting the contributions respectively due to *dynamic*, *friction*, and *kinematic* degrees of freedom in the robot-environment interaction. This matrix is assumed to be full *column* rank, at least in the region of interest for the task execution. Its columns are generalized directions used as a basis for the vector space of the admissible end-effector velocities.

Equations (1) and (2), written for each robot separately, can be rewritten for the whole robotic system as

$$\mathbf{p} = \mathbf{k}(\mathbf{q}) = \mathbf{\Gamma}(\mathbf{s}), \qquad \mathbf{v} = \mathbf{J}(\mathbf{q})\dot{\mathbf{q}} = \mathbf{T}(\mathbf{s})\dot{\mathbf{s}}, \tag{3}$$

where $\mathbf{q} = (\mathbf{q}_1, \mathbf{q}_2)$, $\mathbf{p} = (\mathbf{p}_1, \mathbf{p}_2)$, $\mathbf{v} = (\mathbf{v}_1, \mathbf{v}_2)$, $\mathbf{s} = (\mathbf{s}_{LD}, \mathbf{s}_{F_1}, \mathbf{s}_{F_2}, \mathbf{s}_{K_1}, \mathbf{s}_{K_2})$, $\mathbf{k} = (\mathbf{k}_1, \mathbf{k}_2)$, $\mathbf{\Gamma} = (\mathbf{\Gamma}_1, \mathbf{\Gamma}_2)$, and

$$\mathbf{J} = \begin{bmatrix} \mathbf{J}_1 & \mathbf{O} \\ \mathbf{O} & \mathbf{J}_2 \end{bmatrix}, \quad \mathbf{T} = \begin{bmatrix} \mathbf{T}_{D_1} & \mathbf{T}_{F_1} & \mathbf{O} & \mathbf{T}_{K_1} & \mathbf{O} \\ \mathbf{T}_{D_2} & \mathbf{O} & \mathbf{T}_{F_2} & \mathbf{O} & \mathbf{T}_{K_2} \end{bmatrix} = [\,\mathbf{T}_D\; \mathbf{T}_F\; \mathbf{T}_K\,]. \tag{4}$$

2.2 Statics

The generalized forces exchanged between the ith end-effector and the payload are collected in a g_i-dimensional vector $\mathbf{F}_i$ of forces and torques. In a dual way with respect to (3), the vector of all contact forces $\mathbf{F} = (\mathbf{F}_1, \mathbf{F}_2)$ can be parameterized as $\mathbf{F} = \mathbf{Y}(\mathbf{s})\lambda$. The columns of matrix $\mathbf{Y}$ are generalized directions used as a basis for the vector space of the contact forces. They are such that $\mathbf{T}_K^{\mathrm{T}}\mathbf{Y} = \mathbf{0}$, since contact forces do not perform work on kinematic degrees of freedom. Matrix $\mathbf{Y}$ is assumed to be full rank, and thus the dimension of the vector of force parameters λ will be $g - k$ (with $g = g_1 + g_2$, $k = k_1 + k_2$), namely the difference between the total number of dofs of the end-effectors and the total number of kinematic dofs.

At each $\mathbf{s}$, the vector space of contact forces, *span*$[\mathbf{Y}(\mathbf{s})]$, can be decomposed into two subspaces. The subspace *span*$[\mathbf{Y}_R(\mathbf{s})]$ of reaction forces, i.e., those forces which do not cause payload motion, is such that $[\mathbf{T}_D\; \mathbf{T}_K]^{\mathrm{T}}\,\mathbf{Y}_R = \mathbf{0}$ and has dimension $g - k - d$. Note that the generalized forces in *span*$[\mathbf{Y}_R(\mathbf{s})]$ may perform work on the $\mathbf{s}_F$ variables, hence $\mathbf{T}_F^{\mathrm{T}}\mathbf{Y}_R \neq \mathbf{0}$ in general. The subspace *span*$[\mathbf{Y}_A(\mathbf{s})]$, defined as the complement of $\mathbf{Y}_R$ in $\mathbf{Y}$, is the d-dimensional subspace of active forces responsible for payload motion. Any matrix $\mathbf{Y}_A$, whose columns are used as a basis for this subspace, is such that $\mathbf{T}_D^{\mathrm{T}}\mathbf{Y}_A$ is nonsingular. Following the decomposition of $\mathbf{Y}(\mathbf{s})$, $\mathbf{Y} = [\mathbf{Y}_A\, \mathbf{Y}_R]$, a partition is induced on the parameter vector $\lambda = (\lambda_A, \lambda_R)$. We call in the sequel *dynamic directions* those in the span of the columns of either $\mathbf{T}_D$ or $\mathbf{Y}_A$.

Any choice satisfying the above properties is generally admissible for matrix $\mathbf{Y}$ and, correspondingly, for matrices $\mathbf{Y}_R$ and $\mathbf{Y}_A$. On the other hand, the available freedom in this choice can be used to achieve a physical correspondence of the components of λ with either forces or torques. In particular, λ can be normalized so that the components of λ_R represent the so-called *internal forces* in the robot-payload interaction, while λ_A are the net active forces producing motion of the payload. We recognize that different choices of $\mathbf{Y}$ correspond, for a given task, to different load distributions among the manipulators. From a control point of view, choosing one of the admissible forms for $\mathbf{Y}$ is equivalent to imposing a given load distribution among the robots.

Some further considerations are needed in the presence of friction. In the generalized directions along which friction is effective, a general relation of the form $\Phi(\mathbf{s}_F, \dot{\mathbf{s}}_F, \lambda) = \mathbf{0}$ holds between the generalized coordinates $\mathbf{s}_F$, their derivatives and the parametrization of the generalized contact forces λ. For simplicity, suppose that the grasp is capable to compensate the friction forces arising at the moving contact points (*force closure*). In this case, $\mathbf{Y}$ can be chosen so that all generalized friction forces are parametrized by some components of the subvector λ_R alone. This natural choice implies that friction will not be used for achieving payload motion. Then, we model the friction at the contact points through the following f-dimensional equation (with $f = f_1 + f_2$):

$$\lambda_{R_F} = \mu_F(\mathbf{s}_F, \lambda_{R_P}, \lambda_A) + \nu_F(\mathbf{s}_F, \lambda_{R_P}, \lambda_A)\dot{\mathbf{s}}_F, \tag{5}$$

where $\lambda_R = (\lambda_{R_F}, \lambda_{R_P})$ has been partitioned so that the f-dimensional subvector λ_{R_F} parametrizes the generalized friction forces. The functions μ_F and ν_F model *dry* and *viscous* friction, respectively. Following the decomposition of λ_R, a partition is induced on $\mathbf{Y}_R = [\mathbf{Y}_{R_F}\ \mathbf{Y}_{R_P}]$. As a result, $span[\mathbf{Y}_{R_P}(\mathbf{s})]$ is the subspace of generalized contact forces that do not perform work on any degree of freedom, while forces in $span[\mathbf{Y}_{R_F}(\mathbf{s})]$ perform work only on the $\mathbf{s}_F$ variables. Thus, matrix $\mathbf{Y}_{R_F}$ will be such that $\mathbf{T}_F^{\mathrm{T}}\mathbf{Y}_{R_F}$ is square and nonsingular.

2.3 Dynamics

Following the Lagrangian approach, the dynamic model of the overall system of two robots and payload can be written in the standard form as

$$\mathbf{B}(\mathbf{q})\ddot{\mathbf{q}} + \mathbf{n}(\mathbf{q}, \dot{\mathbf{q}}) = \mathbf{u} - \mathbf{J}^{\mathrm{T}}(\mathbf{q})\mathbf{F}, \tag{6}$$

$$\mathbf{B}_L(\mathbf{s}_{LD})\ddot{\mathbf{s}}_{LD} + \mathbf{n}_L(\mathbf{s}_{LD}, \dot{\mathbf{s}}_{LD}) = \mathbf{T}_D^{\mathrm{T}}(\mathbf{s})\mathbf{F}, \tag{7}$$

with forces $\mathbf{F} = \mathbf{Y}(\mathbf{s})\lambda$ acting from the robots to the object and where

$$\mathbf{B}(\mathbf{q}) = \begin{bmatrix} \mathbf{B}_1 & \mathbf{O} \\ \mathbf{O} & \mathbf{B}_2 \end{bmatrix}, \quad \mathbf{n}(\mathbf{q}, \dot{\mathbf{q}}) = \begin{bmatrix} \mathbf{n}_1 \\ \mathbf{n}_2 \end{bmatrix}, \quad \mathbf{u} = \begin{bmatrix} \mathbf{u}_1 \\ \mathbf{u}_2 \end{bmatrix},$$

with the usual definitions of inertia, Coriolis, centrifugal, and gravity terms.

The couplings between the dynamics of the robots and of the payload are given by the constraints (3) on the end-effectors pose and velocity. In order to obtain a more compact dynamic model that is useful for control purposes, the joint accelerations $\ddot{\mathbf{q}}$ can be explicited from the robots dynamic model (6), and substituted in the differentiated expression of the contact constraints (3). Two alternatives are then available, corresponding to the elimination of the accelerations $\ddot{\mathbf{s}}_{LD}$ or, respectively, of the active forces λ_A from the model equations. In fact, we can explicit one of these two sets of motion and force parameters in terms of the other (and of $\mathbf{s}_K$ and $\mathbf{s}_F$), using the dynamic model of the payload (7). Due to the definition of $\mathbf{s}_{LD}$ and λ_A, both choices are always feasible. When friction is present at the contact, the friction model (5) can be used to further eliminate the explicit appearance of λ_{R_F} in the dynamic equations.

As a result, we obtain the following alternative forms for system description:

$$\mathbf{Q}(\mathbf{q},\mathbf{s}) \begin{bmatrix} \lambda_A \\ \lambda_{R_P} \\ \ddot{\mathbf{s}}_F \\ \ddot{\mathbf{s}}_K \end{bmatrix} = \mathbf{m}(\mathbf{q},\dot{\mathbf{q}},\mathbf{s},\dot{\mathbf{s}}) + \mathbf{J}\mathbf{B}^{-1}\mathbf{u}, \tag{8}$$

$$\widehat{\mathbf{Q}}(\mathbf{q},\mathbf{s}) \begin{bmatrix} \ddot{\mathbf{s}}_{LD} \\ \lambda_{R_P} \\ \ddot{\mathbf{s}}_F \\ \ddot{\mathbf{s}}_K \end{bmatrix} = \widehat{\mathbf{m}}(\mathbf{q},\dot{\mathbf{q}},\mathbf{s},\dot{\mathbf{s}}) + \mathbf{J}\mathbf{B}^{-1}\mathbf{u}. \tag{9}$$

All the involved matrices and vectors depend on the dynamic models of the robots and the payload, and on the chosen parametrization of the system motion. In particular, $\mathbf{m}$ and $\widehat{\mathbf{m}}$ depend also on the friction model through μ_F and ν_F. Examples of the actual form of the terms in eqs. (8) and (9) can be found in [7]. It can be shown that, under mild hypotheses, both $\mathbf{Q}$ and $\widehat{\mathbf{Q}}$ are nonsingular.

Equations (8) and (9) serve as a basis for the design of model-based hybrid motion/force controllers. In particular, by means of an input-output nonlinear control law, we can impose desired and independent evolutions either to the set $(\lambda_A, \lambda_{R_P}, \mathbf{s}_F, \mathbf{s}_K)$ or to the set $(\mathbf{s}_{LD}, \lambda_{R_P}, \mathbf{s}_F, \mathbf{s}_K)$ (see also [11]).

3. APPLICATION TO AN EXPERIMENTAL ROBOTIC CELL

In this section the described formalism is applied to the modeling of a cell with two cooperating robots, available at DIS for experiments in mechanical finishing. The cell consists of a 6-dof parallel platform (SmartEE Hughes) and a 4-dof SCARA-type serial manipulator (IBM 7545), both equipped with an ATI force/torque sensor at their end. The platform can be arbitrarily positioned and oriented in its workspace, so $g_{r_1} = g_{o_1} = 3$ and $g_1 = 6$. Its end-effector is assumed coincident with the center of the top plate. The SCARA end-effector can reach any point in its cartesian workspace, while it can only rotate about the fixed Z axis (normal to the basement plane). Hence, $g_{r_2} = 3$, $g_{o_2} = 1$, and $g_2 = 4$. A total of $g = 10$ end-effector dofs are involved. A CAD picture of the cell is shown in Fig. 1.

The typical task can be described as follows. The payload is a rigid object (*workpiece*) of general but smooth form carried by the SmartEE platform and rigidly attached to it. The platform can be arbitrarily positioned and oriented in its workspace. The SCARA end-effector is equipped with a milling tool that moves in contact with the object surface. The orientation of the tool is constrained to a single direction because of the limited degrees of freedom of the SCARA arm. The interaction between tool and workpiece can be modeled as a point contact. In this interaction normal and tangential forces arise, the latter being caused by the existing friction in the sliding motion. Forces and torques acting on the workpiece can be measured at the contacts with the SCARA and with the SmartEE respectively, through the two 6D-sensors. The joint positions of the two robots are measured with encoders. The mechanical finishing operation requires a prescribed motion trajectory of the tool on the workpiece surface while controlling the exerted normal force.

Fig. 1: CAD picture of the experimental robotic cell at DIS

The object can move in the free space within the described grasp configuration, so that $l = 6$. The vector $\mathbf{s}_L$ can be chosen as

$$\mathbf{s}_L = (\mathbf{r}_O, \mathbf{e}_O), \tag{10}$$

being $\mathbf{r}_O$ the absolute position of the workpiece center of mass and $\mathbf{e}_O$ a minimal representation of the orientation of a frame attached to it. The payload has no extra dofs (its pose is completely determined by the positions of the contact points with the two robots), so that $\mathbf{s}_L = \mathbf{s}_{LD}$ and $l = d$.

As the workpiece is rigidly grasped by the platform, the dynamic variables $\mathbf{s}_{LD}$ uniquely determine the pose $\mathbf{p}_1$ of the platform, yielding $f_1 = k_1 = 0$. Three other variables are needed instead to identify the SCARA end-effector pose, as its position on the object surface and its orientation vary during the task. In particular, we need two local coordinates defined on the object surface and the absolute orientation of the SCARA end-effector about the fixed Z axis. Friction forces act tangentially to the contact surface, while we assume that the friction torque about the normal direction is negligible. Thus, the two surface coordinates are collected in the vector $\mathbf{s}_F$ of friction variables, while the orientation angle is the single kinematic variable s_K. Hence, $f = f_2 = 2$, $k = k_2 = 1$, $\mathbf{s} = (\mathbf{s}_{LD}, \mathbf{s}_F, s_K) \in I\!R^9$, and

$$\mathbf{p}_1 = \begin{bmatrix} \mathbf{r}_O + {}^B\mathbf{R}_O(\mathbf{e}_O)\,{}^O\mathbf{r}_{c_1} \\ \mathbf{e}\,({}^B\mathbf{R}_O(\mathbf{e}_O)\,{}^O\mathbf{R}_{R_1}) \end{bmatrix} = \boldsymbol{\Gamma}_1(\mathbf{s}), \tag{11}$$

$$\mathbf{p}_2 = \begin{bmatrix} \mathbf{r}_O + {}^B\mathbf{R}_O(\mathbf{e}_O)^O\mathbf{r}_{c_2}(\mathbf{s}_F) \\ s_K \end{bmatrix} = \mathbf{\Gamma}_2(\mathbf{s}), \tag{12}$$

where ${}^B\mathbf{R}_O(\mathbf{e}_O)$ is the rotation matrix representing the orientation of the object with respect to the base frame, ${}^O\mathbf{R}_{R_1}$ defines the *constant* relative orientation between the frame attached to the object and the platform end-effector, ${}^O\mathbf{r}_{c_i}$ is the vector locating the ith contact point in the object frame, and $\mathbf{e}(\mathbf{R})$ is a 3-dimensional vector that extracts a minimal representation of the orientation from the rotation matrix $\mathbf{R}$. From (11) and (12), it follows

$$\mathbf{v}_1 = \begin{bmatrix} \mathbf{I}_{3\times3} & \frac{\partial}{\partial \mathbf{e}_O}\left[{}^B\mathbf{R}_O(\mathbf{e}_O)^O\mathbf{r}_{c_1}\right] \\ \mathbf{O}_{3\times3} & {}^B\mathbf{R}_O(\mathbf{e}_O)^O\mathbf{K}(\mathbf{e}_O) \end{bmatrix} \begin{bmatrix} \dot{\mathbf{r}}_O \\ \dot{\mathbf{e}}_O \end{bmatrix} = \mathbf{T}_{D_1}(\mathbf{s}_{LD})\dot{\mathbf{s}}_{LD}, \tag{13}$$

$$\begin{aligned} \mathbf{v}_2 &= \begin{bmatrix} \mathbf{I}_{3\times3} & \frac{\partial}{\partial \mathbf{e}_O}\left[{}^B\mathbf{R}_O(\mathbf{e}_O)^O\mathbf{r}_{c_2}(\mathbf{s}_F)\right] \\ \mathbf{0}_{1\times3} & \mathbf{0}_{1\times3} \end{bmatrix} \begin{bmatrix} \dot{\mathbf{r}}_O \\ \dot{\mathbf{e}}_O \end{bmatrix} + \begin{bmatrix} {}^B\mathbf{R}_O(\mathbf{e}_O)\frac{\partial {}^O\mathbf{r}_{c_2}(\mathbf{s}_F)}{\partial \mathbf{s}_F} & \mathbf{0}_{3\times1} \\ \mathbf{0}_{1\times2} & 1 \end{bmatrix} \begin{bmatrix} \dot{\mathbf{s}}_F \\ \dot{s}_K \end{bmatrix} \\ &= \mathbf{T}_{D_2}\dot{\mathbf{s}}_{LD} + \mathbf{T}_{F_2}\dot{\mathbf{s}}_F + \mathbf{T}_{K_2}\dot{s}_K. \end{aligned} \tag{14}$$

where ${}^O\mathbf{K}(\mathbf{e}_O)\dot{\mathbf{e}}_O$ is the angular velocity of the object (expressed in the object frame).

Being $\mathbf{T}_D$, $\mathbf{T}_F$, and $\mathbf{T}_K$ defined by the above equations, feasible choices for the (10×3) matrix $\mathbf{Y}_R$ and the (10×6) matrix $\mathbf{Y}_A$ in the contact force parametrization $\mathbf{F} = \mathbf{Y}_R(\mathbf{s})\lambda_R + \mathbf{Y}_R(\mathbf{s})\lambda_R$ are given by:

$$\mathbf{Y}_R = \begin{bmatrix} -{}^B\mathbf{R}_{sur}(\mathbf{s}_{LD}, \mathbf{s}_F) \\ {}^B\mathbf{R}_O(\mathbf{e}_O)\mathbf{S}[\mathbf{r}_{c_1} - \mathbf{r}_{c_2}(\mathbf{s}_F)]{}^B\mathbf{R}_O^{\mathrm{T}}(\mathbf{e}_O){}^B\mathbf{R}_{sur}(\mathbf{s}_{LD}, \mathbf{s}_F) \\ {}^B\mathbf{R}_{sur}(\mathbf{s}_{LD}, \mathbf{s}_F) \\ \mathbf{0}_{1\times3} \end{bmatrix}, \tag{15}$$

$$\mathbf{Y}_A = \begin{bmatrix} \mathbf{I}_{3\times3} & \mathbf{O}_{3\times3} \\ -{}^B\mathbf{R}_O(\mathbf{e}_O)\mathbf{S}[\mathbf{r}_{c_1}]{}^B\mathbf{R}_O^{\mathrm{T}}(\mathbf{e}_O) & \mathbf{I}_{3\times3} \\ \mathbf{O}_{4\times3} & \mathbf{O}_{4\times3} \end{bmatrix}. \tag{16}$$

Here, ${}^B\mathbf{R}_{sur}(\mathbf{s}_{LD}, \mathbf{s}_F) = {}^B\mathbf{R}_O(\mathbf{s}_{LD})^O\mathbf{R}_{sur}(\mathbf{s}_F)$ defines the relative orientation between the base frame and a frame attached to the object surface, having its origin at the point identified by $\mathbf{s}_F$, with the $X_{sur} - Y_{sur}$ coordinate plane tangent to the contact surface, and with the Z_{sur} axis along the (ingoing) normal to the surface. Moreover, $\mathbf{S}[\mathbf{r}]$ is the skew-symmetric matrix generated by a vector $\mathbf{r}$.

With the above choices of $\mathbf{Y}_R$ and $\mathbf{Y}_A$, $\lambda_A \in I\!R^6$ is the parametrization of the active forces on the object expressed in the base frame, while $\lambda_R \in I\!R^3$ —the parametrization of the internal forces— coincides with the contact force exerted by the SCARA robot expressed in the frame characterized by ${}^O\mathbf{R}_{sur}$ at the contact point (*task frame*). In particular, the first two components of λ_R parametrize the contact force acting tangentially to the object surface (i.e., the friction force), while the third component represents the force exerted by the SCARA robot along the normal to the surface. Hence, $\lambda_{R_F} = (\lambda_{R_1}, \lambda_{R_2})$ and $\lambda_{R_P} = \lambda_{R_3}$, according to the definitions in Sect. 2.2.

As friction is a relevant phenomenon in the task we are interested in, a reliable friction model should be adopted. In [12], an experimentally validated description of friction in deburring tasks is proposed. Using the described formalism, it can be expressed as

$$\lambda_{R_F} = \lambda_{R_P} \mathbf{K}_F \dot{\mathbf{s}}_F, \tag{17}$$

where $\mathbf{K}_F$ is a diagonal matrix of friction coefficients (constant in the region of task execution). As previously indicated, eq. (17) can be used to eliminate the appearance of λ_{R_F} in the model equations.

As a result of the modeling phase, we may use e.g. the description (9) to define a hybrid controller of the ten quantities $\mathbf{s}_{LD}$, $\mathbf{s}_F$, s_K (nine motion parameters), and λ_{R_P} (one force parameter).

4. CONCLUSION

We have presented a task-oriented modeling approach for general cooperating robot systems and its specific application to a cell with two different robots involved in a mechanical finishing operation. The proposed formalism is useful for control purposes because it leads to a system description in terms of the kinematic and dynamic quantities that characterize the task. Thus, generalized hybrid motion/force controllers can be directly designed (see, e.g., [7] and [11]) starting from the obtained model of the system.

REFERENCES

[1] J.Y.S. Luh and Y.F. Zheng, "Constrained relations between two coordinated industrial robots for motion control," *Int. J. of Robotics Research*, Vol. 6, No. 3, pp. 60–70, 1987.

[2] T. Yoshikawa and X. Zheng, "Coordinated dynamic hybrid position-force control for multiple robot manipulators handling one constrained object," *1990 Int. Conf. on Robotics and Automation*, Cincinnati, OH, pp. 1178–1183, 1990.

[3] T.J. Tarn, A.K. Bejczy, and X. Yun, "New nonlinear control algorithms for multiple robot arms," *IEEE Trans. on Aerospace and Electronic Systems*, Vol. 24, No. 5, pp. 571–583, 1988.

[4] F.-T. Cheng and D.E. Orin, "Efficient algorithm for optimal force distribution—The compact-dual LP method," *IEEE Trans. on Robotics and Automation*, Vol. 6, No. 2, pp.178–187, 1990.

[5] H. Bruhm, J. Deisenroth, and P. Schädler, "On the design and simulation-based validation of an active compliance law for multi-arm robots," *Robotics and Autonomous Systems*, Vol. 5, pp. 307–321, 1989.

[6] C. von Albrichsfeld, M. Svinin, and H. Tolle, "Learning approach to the active compliance control of multi-arm robots coupled through a flexible object," *3rd European Control Conf.*, Roma, I, pp. 1900–1905, 1995.

[7] A. De Luca and R. Mattone, "Modeling and control for cooperating robots handling payloads with extra degrees of freedom," *3rd European Control Conf.*, Roma, I, pp. 1923–1930, 1995.

[8] R.M. Murray, Z. Li, and S.S. Sastry, *A Mathematical Introduction to Robotic Manipulation,* CRC Press, Boca Raton, 1994.

[9] E. Paljug, X. Yun, and V. Kumar, "Control of rolling contacts in multi-arm manipulation," *IEEE Trans. on Robotics and Automation*, Vol. 10, No. 4, pp. 441–452, 1994.

[10] A. Bicchi and R. Sorrentino, "Dexterous manipulation through rolling," *1995 IEEE Int. Conf. on Robotics and Automation*, Nagoya, J, pp. 452–457, 1995.

[11] A. De Luca and R. Mattone, "Modeling and control alternatives for robots in dynamic cooperation," *1995 IEEE Int. Conf. on Robotics and Automation*, Nagoya, J, pp. 138–145, 1995.

[12] A. Fedele, A. Fioretti, and G. Ulivi, "Experiments in robotic deburring with on-line surface identification," *2nd IEEE Mediterranean Symp. on New Directions in Control and Automation*, Chania, GR, pp. 120–126, 1994.

Missing Fig. 1 at page 6

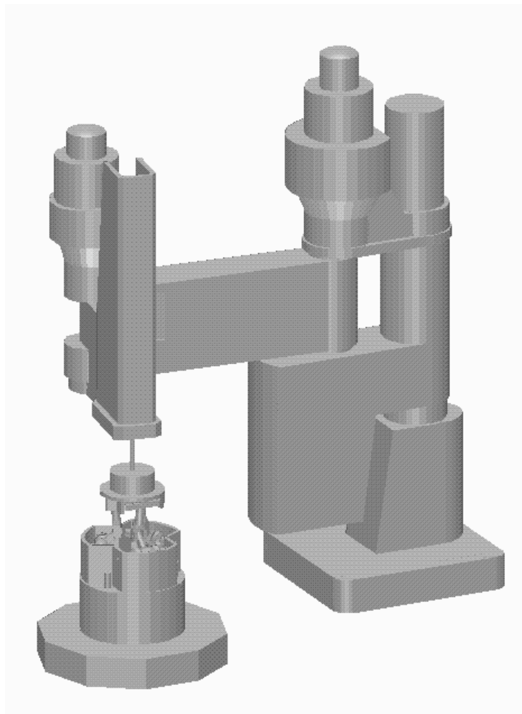

Fig. 1: CAD picture of the experimental robotic cell at DIS